Title: Ribosomal RNA methylation by GidB is a capacitor for discrimination of mischarged tRNA

Authors: Zhuo Bi[1,2], Hong-Wei Su[1], Jia-Yao Hong[1] and Babak Javid[1,3*]

Affiliations:

[1] Center for Global Health and Infectious Disease, Tsinghua University School of Medicine, Beijing, China

[2] School of Life Science, Tsinghua University, Beijing, China

[3] Division of Experimental Medicine, University of California, San Francisco, CA, USA

[*] to whom correspondence should be addressed: babak.javid@ucsf.edu

Summary

Despite redundant cellular pathways to minimize translational errors, errors in protein synthesis are common. Pathways and mechanisms to minimize errors are classified as pre-ribosomal or ribosomal. Pre-ribosomal pathways are primarily concerned with appropriate pairing of tRNAs with their cognate amino acid, whereas to date, ribosomal proof-reading has been thought to only be concerned with minimizing decoding errors, since it has been assumed that the ribosomal decoding centre is blind to mischarged tRNAs. Here, we identified that in mycobacteria, deletion of the 16S ribosomal RNA methyltransferase *gidB* led to increased discrimination of mischarged tRNAs. GidB deletion was necessary but not sufficient for reducing mistranslation due to misacylation. Discrimination only occurred in mycobacteria enriched from environments or genetic backgrounds with high rates of mistranslation. Our data suggest that mycobacterial ribosomes are capable of discriminating mischarged tRNAs and that 16S rRNA methylation by GidB may act as a capacitor for moderating translational error.

Introduction

All cells in all clades of life have evolved multiple, redundant pathways to reduce translational error [1, 2]. Yet errors in protein synthesis are remarkably common and are orders of magnitude more frequent than errors in DNA or RNA synthesis [3-7]. There is no one 'optimal' rate of error. Tolerable error rates are both species and even organelle specific [1, 8], and the major source of errors vary by mechanism and species [1]. Furthermore, translational errors, mistranslation, may result in adaptive phenotypes, particularly in the context of environmental stressors [1, 5, 6, 9-20]. However, excess mistranslation can also cause protein aggregation [21, 22], organ degeneration [23, 24] and is the mechanism for the bactericidal activity of aminoglycosides [25], suggesting that an optimal balance for translational error does exist, but one that is tunable and context specific [1, 3, 5, 26].

In addition, molecular mechanisms of translational error whether physiological or undesirable vary considerably, as do the proof-reading pathways that have evolved to reduce them. Generally, sources of error and proof-reading can be divided into pre-ribosomal and ribosomal mechanisms [1]. Pre-ribosomal proof-reading mechanisms include pre- and post-transfer editing functions of aminoacyl tRNA synthetases [27]. Following aminoacyl-tRNA synthesis, *trans*-acting editing mechanisms can reject mischarged tRNAs [28, 29], and the aminoacyl-tRNA chaperone, EF-Tu optimally binds cognate aminoacyl-tRNAs compared with mischarged tRNAs [30]. These multiple and redundant pre-ribosomal proof-reading steps – solely concerned with the cognate pairing of the aminoacyl group to its tRNA – have been proposed as necessary since ribosomal proof-reading mechanisms to date have exclusively been concerned with ensuring cognate codon·anticodon pairing [2, 31].

Regardless of these multiple proof-reading mechanisms, translational fidelity is relative [6, 32]. Most bacteria with the notable exception of a few proteo-bacteria such as *Escherichia coli* lack either the glutaminyl- or asparaginyl-tRNA synthetases, or both [33]. Instead, a two-step indirect tRNA synthesis pathway, in which non-discriminatory glutamyl or aspartyl synthetases mischarge glutaminyl-tRNA with glutamate and asparaginyl-tRNA with aspartate respectively in the first step is used. At least in mycobacteria (which lack both synthetases), this results in baseline error rates specifically of glutamine

to glutamate and asparagine to aspartate orders of magnitude higher than measured in *E. coli* [17, 34]. The critical enzyme in the second step of the indirect pathway is GatCAB, whose function is to correct the mischarged aminoacyl moiety [35]. Despite its essential function, partial loss-of-function mutations in *gatCAB* can be readily selected in mycobacteria, occur naturally in clinical isolates of pathogenic *M. tuberculosis* [12, 36], and these mutant strains exhibit extremely high (up to 10%/codon) but specific rates of mistranslation [12]. Here, we investigated whether further fidelity factors can be identified in mycobacteria. We identified that the 16S ribosomal RNA (rRNA) methyltransferase *gidB* is necessary but not sufficient for discrimination of mischarged tRNAs in mycobacteria. Deletion of *gidB* only increased discrimination of misacylated tRNAs in mycobacteria with elevated mistranslation rates – due to mutation or environmental context – suggesting that non-methylation of rRNA may act to prevent catastrophic translational error.

Results

A suppressor screen in mycobacteria identifies *gidB* as a potential translational fidelity factor

We had previously identified via forward genetic screens strains of *Mycobacterium smegmatis* with extremely high specific rates of mistranslation due to mutations in the essential amidotransferase genes *gatCAB* [12, 36]. We hypothesized that the mycobacterial genome may encode for other 'fidelity factors' that may either enhance or reduce mistranslation specifically involving the indirect tRNA aminoacylation pathway. We designed a suppressor screen strategy on the background of a high mistranslator strain (Fig 1A). We focused on one strain, HWS19, with a three amino acid deletion in *gatA*, since this mutation caused the strain to have extremely high rates of translational error [12]. Aminoglycosides such as streptomycin are known to increase ribosomal decoding errors [37, 38], and we wondered whether HWS19, with a high background mistranslation rate, but due to a different (pre-ribosomal) mechanism, is also more susceptible to streptomycin. Plating of equivalent colony forming units (CFU) of strain HWS19 on low-dose streptomycin-agar led to recovery of significantly fewer colonies compared with wild-type (Fig. S1), confirming HWS19 was hypersusceptible to streptomycin. The basis of our suppressor screen, therefore, was as follows: plating of HWS19 onto low-dose streptomycin-agar should select for strains with mutations that *decrease* mistranslation on this high

mistranslating background (Fig. 1A, B). We plated $1x10^7$ CFU onto each of 6 agar plates containing 1 µg/mL streptomycin. We sequenced the *rpsL* gene of survivors to exclude mutants that arose due to *de novo* resistance to streptomycin. Remaining survivors were transformed with a dual-luciferase reporter plasmid that measured specific mistranslation errors of asparagine for aspartate [12, 17, 39] to identify low mistranslating candidates (Fig. 1B). We initially identified 4 suppressor mutants with lower mistranslation rates compared with the parent HWS19 strain, and comparable to wild-type *M. smegmatis* (Fig. 1C). Sequencing the strains revealed three had mutations in the 16S rRNA methyltransferase *gidB* (Msmeg_6940) – Table S1. We subsequently sequenced just the *gidB* gene of a further 10 candidates and identified a further seven with a total of three additional independent mutations in *gidB* (Table S2). All but one of these further suppressors also had reduced mistranslation rates (Fig. S2).

Deletion of *gidB* increases discrimination against misacylated tRNA in mycobacteria with high mistranslation

Since loss of function mutations in GidB can cause low-level streptomycin resistance in mycobacteria [40, 41], we were concerned that our candidates from the screen may represent selection against streptomycin. To determine whether the observed phenotype was independent of streptomycin selection, we deleted *gidB* in both the HWS19 and wild-type *M. smegmatis* backgrounds. Deletion strains were complemented with a chromosomally integrated plasmid expressing *gidB* (Fig. S3). We measured specific mistranslation rates using two complementary reporter systems: the dual-luciferase system, used in the initial screen, as well as a dual-fluorescent reporter system (Fig. S4) that uses flow cytometry to measure relative mistranslation rates and [12]. Measurement of specific mistranslation rates with both reporters verified that deletion of *gidB* significantly increased fidelity in strain HWS19, and this phenotype could be readily complemented (Fig. 2A, B). Surprisingly, deletion of *gidB* had no phenotype using the same reporters on a wild-type background (Fig. 2C, D).

Mycobacteria, due to their two-step indirect tRNA aminoacylation pathway physiologically misacylate glutaminyl- and asparaginyl-tRNAs in the first step [12, 35]. We wanted to investigate whether deletion

of *gidB* in *Escherichia coli*, which does not employ the two-step pathway, and instead codes for the full set of 20 aminoacyl tRNA synthetases had a high fidelity phenotype. To mimic the high mistranslating environment of strain HWS19, we transformed the *E. coli* strain HK295 with one of two plasmids encoding non-discriminatory aminoacyl tRNA synthetases (ND-aaRSs): a non-specific aspartyl synthetase from *Deinococcus radiodurans*, that mischarges *E. coli* asparaginyl-tRNA with aspartate [10, 32]; and a non-discriminatory glutamyl synthetase from *Bacillus subtilis* that mischarges *E. coli* glutaminyl-tRNA with glutamate [32]. Induction of the ND-aaRSs resulted in substantially elevated specific mistranslation rates in *E. coli*, as demonstrated previously [32]. However, deletion of *gidB* (Fig. S5) did not result in increased discrimination of these misacylated tRNAs (Fig. 2E, F).

GidB is necessary for discrimination of mischarged tRNA under conditions that enrich for relatively high mistranslation rates

Deletion of *gidB* only had a phenotype under standard laboratory conditions in a high mistranslating mycobacterial mutant. Therefore, we decided to enrich isogenic populations of wild-type mycobacteria that have higher mistranslation rates than when grown under standard laboratory conditions and test whether *gidB*-deletion had a phenotype under these conditions. We used a reporter in which the kanamycin kinase gene *aph* had been mutated at a critical aspartate residue that rendered it inactive, Aph-D214N [17, 42, 43]. Mycobacteria, including wild-type mycobacteria, expressing this reporter could survive in low-dose kanamycin due to the high basal (~ 1%/codon bulk average) mistranslation of asparagine to aspartate [12], which would reconstitute a small proportion of fully active kanamycin kinase (Aph-N214D, i.e. wild-type enzyme). We compared the relative mistranslation rates of wild-type and *gidB*-deleted (on wild-type background) bacteria scraped from non-selective LB-agar or low-dose kanamycin agar. As before, *gidB*-deletion had no effect on the mistranslation rate on bacteria isolated from LB-agar. The average mistranslation rate of bacteria scraped from kanamycin-agar was higher, as predicted. In addition, from this context, deletion of *gidB* significantly increased translational fidelity (Fig. 3A).

We were unable to complement the strain in this experiment due to lack of appropriate selection markers. We therefore decided to test wild-type mycobacteria in a further environmental condition known to enrich for relatively high mistranslation rates. We had previously shown that a substantial minority of wild-type mycobacteria could survive and grow in bulk-lethal concentrations of rifampicin, due to two reversible and non-genetic mechanisms: increased mistranslation [12] and a semi-heritable survival programme [44] and not due to mutations causing *bona fide* rifampicin resistance. We plated bacteria on non-selective medium or rifampicin-agar. As before, Δ*gidB* isolated from non-selective medium had no phenotype. However, bacteria that survived and grew on rifampicin-agar had increased rates of mistranslation, which reverted with deletion of *gidB*, in a fully complementable manner (Fig. 3B). To investigate whether deletion of *gidB* was sufficient for discrimination of mischarged tRNA in cells with higher mistranslation rates we re-analyzed bacteria with the highest (10%) and lowest (10%) green/red (i.e. relative mistranslation rates) ratios from the two experiments. Deletion of *gidB* had no observable phenotype on translational fidelity in bacteria isolated from non-selective media, even when only the cells with the highest apparent mistranslation rates were analysed (Fig. 3C,D), unlike bacteria enriched for higher mistranslation rates. Therefore, *gidB* deletion appears necessary, but not sufficient for translational fidelity, and it is only within environmental contexts that enrich for high rates of mistranslation that deletion of *gidB* causes increased ribosomal discrimination of misacylated tRNA in otherwise wild-type mycobacteria.

Deletion of *gidB* increased discrimination of physiologically mischarged Glu-tRNA^{Gln}. However, was discrimination of mischarged tRNA confined to misacylated tRNAs that would be encountered physiologically, or was it a general property that would allow discrimination of any mischarged tRNA, regardless of whether such a moiety would be encountered within a ‘natural’ context? We exploited the unique properties of alanyl tRNAs and their cognate synthetase. Unlike most aminoacyl tRNA synthetases, alanyl synthetase (AlaRS), does not rely on the anticodon of its cognate tRNAs as an identity element. The unique, and ubiquitous identity element of alanyl-tRNAs in all clades of life is a G^3·U base-pair in the tRNA acceptor stem [45-47]. This base-pair is necessary and sufficient for recognition and charging of any tRNA by AlaRS. Therefore, the anticodon of any alanyl-tRNA can be

mutated to any triplet, and the tRNA will still be charged with aminoacyl-alanine [45] and will mediate specific translational errors. We had previously mutated the anticodon of a mycobacterial alanyl-tRNA to CCA, coding for tryptophan, which would result in specific mistranslation of alanine for tryptophan at UGG codons [17]. To measure specific mistranslation, we modified the dual-luciferase reporter system. We identified a critical alanine residue in Renilla luciferase, which, when mutated to tryptophan (A214W), resulted in >20-fold decrease in activity (Fig. S6). This reporter would thus be able to discriminate mistranslation errors greater than 5%/codon of tryptophan to alanine. We transformed the mutant alanyl-tRNA ($tRNA_{CCA}^{Ala}$), cloned into a tetracycline-inducible plasmid (termed EMAW – 'excess mistranslation of alanine for tryptophan'), into wild-type and Δ*gidB M. smegmatis*, along with the specific dual-luciferase reporters. Induction of $tRNA_{CCA}^{Ala}$ resulted in increased specific mistranslation of tryptophan for alanine, as expected. Deletion of *gidB* did not increase translational fidelity, even in this high mistranslating context (Fig. 3E). However, transformation of EMAW and reporters into HWS19 confirmed that in this strain with high rates of 'physiological' mistranslation, deletion of *gidB* allowed ribosomes to further discriminate against even non-physiologically mischarged tRNAs (Fig. 3F). Taken together, these results suggested deletion of *gidB* was necessary but not sufficient for discrimination of mischarged tRNAs and that a further environmental context, possibly generated via excess 'physiological' mistranslation or some other stressor was also required.

Deletion of *gidB* causes reduced tolerance to rifampicin

Finally, we wished to test the potential physiological relevance of increased translational fidelity caused by *gidB* deletion. We had previously demonstrated that increased, specific, mistranslation due to the mycobacterial indirect tRNA aminoacylation pathway caused increased tolerance to the antibiotic rifampicin due to mistranslation of critical residues in the drug target, RpoB [12, 17]. Since antibiotic tolerance is mediated by a subpopulation of bacteria that resist killing [48-58], we hypothesised that deletion of *gidB* would render the most tolerant subpopulation susceptible to rifampicin. Measuring survival of *M. smegmatis* exposed to rifampicin in axenic culture, deletion of *gidB* resulted in significantly increased killing in both the high mistranslating strain HWS19 and in wild-type mycobacteria (Fig. 3G, H).

Discussion

The ubiquitous presence of multiple and redundant proof-reading mechanisms for protein synthesis underscores the importance of accurate protein synthesis in cellular homeostasis. However, errors in protein synthesis are both more pervasive and frequent than previously anticipated, and increasingly, translational errors are being recognised as a mechanism for adaptation to hostile environments. One possible resolution of these two seemingly opposed processes is the recognition that 'optimal' fidelity is not as low as possible and is context-specific [5, 6, 59]. For example, infection by *Salmonella* mutants with both impaired and enhanced translational fidelity were less productive than wild-type strains [26], and mycobacterial strains with extremely high mistranslation rates due to mutations in *gatA* grew more slowly than wild-type in axenic culture, but had orders of magnitude greater survival with rifampicin treatment [12].

In this study we sought to identify further translational fidelity factors in mycobacteria, which we had previously shown have high, but specific rates of mistranslation due to the indirect tRNA aminoacylation pathway required for aminoacylation of glutaminyl- and asparaginyl-tRNAs [10, 12, 36]. Our screen identified loss-of-function mutations in *gidB* conferring increased fidelity to errors generated by mutants in this pathway. GidB, also called RsmG is a known methyltransferase that confers m^7G methylation to the guanosine at position 507 (*M. smegmatis* numbering) on 16S rRNA [40, 41, 60]. Despite its universal conservation in bacteria [40], it is not essential for *in vitro* growth [60, 61], suggesting critical functions that are not necessary for growth under standard laboratory conditions. We had previously shown that deletion of *gidB* in *M. tuberculosis* increased fidelity of 'wobble' ribosomal decoding errors, but not for mistranslation of asparagine for aspartate – one of the two specific errors in mycobacteria due to the indirect tRNA pathway [41]. Those studies, performed with otherwise wild-type mycobacteria under standard laboratory conditions, mimic similar conditions where in this study *gidB* deletion also lacked a phenotype.

The ribosome has several proof-reading mechanisms [2]. At initial selection of aminoacyl-tRNA and prior to the GTP hydrolysis that catalyzes peptide bond formation, non-cognate (to the mRNA codon) aminoacyl tRNAs are rejected [62]. A second proof-reading step occurs after GTP hydrolysis, but prior to peptide bond formation [31]. A further proof-reading step after peptide bond formation with a non-cognate aminoacyl-tRNA donor can result in abortive termination of protein synthesis [63]. However, all these ribosomal proof-reading mechanisms serve to preserve the accuracy of cognate mRNA codon·tRNA anticodon interactions, whereas mischarged tRNAs, by definition, have cognate codon·anticodon contact. A study of A-site binding of a set of 4 different tRNA backbones each esterified with 4 aminoacyl groups failed to identify a substantial contribution of the aminoacyl identity on ribosome binding [64]. A subsequent study of a more diverse set of tRNAs did find that the ribosomal A site does confer specificity for aminoacyl-tRNAs [65], but did not specifically address the question of proof-reading of misacylated tRNA. Cornish and colleagues used an elegant biochemical approach to investigate interaction of the ribosome with mischarged but otherwise natural tRNAs using di-peptide formation assays and small molecule FRET [66]. Although overall there were few differences in ribosome dynamics between cognately charged and mischarged aminoacyl tRNAs, there were subtle differences in some mischarged tRNAs, notably a small (2-3 fold) increase in A-site sampling by some mischarged tRNAs [66]. This is particularly interesting given the recent description that some aminoacyl tRNA·EF-Tu·GTP ternary complexes repeatedly engage with the ribosome during the second proof-reading step of peptide-bond formation [31]. Our prior studies with the unusual aminoglycoside kasugamycin [10] also suggest ribosomes can discriminate against mischarged tRNAs. Kasugamycin was known to decrease ribosomal decoding errors [67, 68] in direct contrast with the increased errors witnessed with other aminoglycosides such as streptomycin. We showed that kasugamycin, at concentrations that did not inhibit protein synthesis, could decrease mistranslation from mischarged tRNAs not only in live mycobacteria, but also in a cell-free *in vitro* translation system, which had been modified to include excess mischarged Asp-tRNA^{Asn} [10].

We do not know the precise molecular mechanism by which deletion of *gidB* increases ribosomal discrimination of mischarged tRNAs. Given the target methylation site for GidB is located in the

decoding centre, one can conceive a mechanism by which lack of 16S methylation promotes increased resampling of the A-site, and subsequently rejection of mischarged tRNA ternary complexes prior to peptide bond formation. Furthermore, it was notable that deletion of *gidB* was necessary, but insufficient for discrimination of mischarged tRNAs. Only mycobacteria with increased mistranslation rates – either via mutation or from an environmental context in which higher mistranslation rates are favoured – had a high fidelity phenotype in the absence of *gidB*. This extended to discrimination of mischarged tRNAs that are not naturally occurring, such as Ala-$tRNA_{CCA}^{Ala}$. However, deletion of *gidB* did not lead to similar phenotypes in *E. coli*: regardless of whether the bacteria were experiencing high mistranslation rates or not – although the two types of excess mistranslation we tested mimicked the indirect tRNA aminoacylation pathway that is not present in *E. coli*, and hence 'unnatural' in the context of that species. Oxidative stress leads to accumulation of toxic non-coded amino-acids in *E. coli* [69], therefore it is tempting to speculate *gidB* deletion in that context may have a discriminatory phenotype. What further changes to ribosomal composition or function are required for lack of GidB-mediated methylation to effectively discriminate against mischarged tRNAs? We and others have recently described alternative bacterial ribosomes that are particularly adapted to stressful environments – such environments are also associated with relaxation of translational fidelity [70-72]. However, multiple forms of alternative ribosomes have been identified: comprising altered stoichiometry of ribosomal protein subunits, variant subunits or alternative rRNA composition [73, 74]. Which, if any of these alternatives contribute to increased fidelity in absence of GidB-mediated rRNA methylation will be the subject of ongoing study.

Deletion of *gidB* causes increased mycobacterial susceptibility to rifampicin. Since lack of *gidB* decreases both wobble misreading [41], as well as discrimination of mischarged tRNA, which function is responsible? Several lines of evidence suggest discrimination of mischarged tRNAs is more likely. First, we have previously demonstrated that increased discrimination of mischarged tRNA by kasugamycin is responsible for enhanced mycobacterial susceptibility to rifampicin *in vitro* [10]. Secondly, the magnitude of increased susceptibility of *ΔgidB* is greater in strain HWS19, in which the vast majority of error is derived from mischarged tRNA. Finally, the absolute error rates of ribosomal

decoding errors in mycobacteria, including wobble mistranslation, are much lower than for errors due to mischarged tRNA [17, 38], making the latter mechanism more parsimonious.

Emerging data suggest absolute fidelity in protein synthesis is not desirable, not only from an efficiency perspective, but also because relaxed fidelity is associated with adaptation to hostile environments. Although moderate mistranslation rates may be adaptive under stress, excessive mistranslation is still harmful. Therefore, mechanisms that are permissive for moderate but not excessive mistranslation may serve an important function in bacterial environmental adaptation. Ribosomal RNA methylation may be reversible [75], although definitive evidence is not available. Since lack of methylation by GidB is only effective at increasing ribosomal discrimination against mischarged tRNA under contexts of high mistranslation, it may serve as a brake for runaway mistranslation and error catastrophe.

MATERIALS AND METHODS

Bacterial strains and culture

Wild-type *M. smegmatis* mc^2-155 [76] and its derivatives were cultured in Middlebrook 7H9 Broth supplemented with 0.2% glycerol, 10% ADS (albumin-dextrose-salt) and 0.05% Tween-80 with corresponding antibiotics. Wild-type *E. coli* HK295 and its derivatives were cultured in LB Broth with corresponding antibiotics. *E. coli* DH5α and TOP10 were used for transformation of plasmids and amplification. LB-Agar was used for both *M. smegmatis* and *E. coli* in plating experiments. If not otherwise mentioned, bacteria were grown in 37 ℃, 220 rpm shaker or maintained in 37℃ incubator.

Suppressor screen.

A total of around $1x10^7$ colony forming units (C.F.U) HWS19 were plated onto each of 6 LB agar plates containing 1μg/mL streptomycin. After 5 days, visible colonies were picked for further analysis. The *rpsL* gene was amplified by PCR and sequenced, those with wild-type *rpsL* were transformed with Renilla-Firefly dual luciferase reporter plasmids (Renilla-Firefly WT and Renilla-Firefly D214N). Specific mistranslation rates of asparagine for aspartate were measured in potential suppressor candidates to identify low mistranslating strains compared with HWS19. Genomic DNA was isolated from HWS19 and four suppressor candidates by standard methods, and were then whole-genomes sequenced and analyzed by Genewiz. The whole genome sequence data have been deposited to the NCBI short-read archive <https://www.ncbi.nlm.nih.gov/sra> with accession number: PRJNA704242. Mapping results of mutations onto genes covering over 99% of all reads in four suppressor candidates are shown as Table S1. A further 10 suppressor candidates had only *gidB* sequenced as per Table S2.

Deletion of *gidB* and complementation in *Mycobacterium smegmatis*

The 500 bp upstream and downstream regions of *gidB* were amplified from mc^2-155 genomic DNA. The zeocin resistance cassette was amplified from plasmid pKM-Zeo-Lox (A kind gift from Eric J. Rubin lab). Then the zeocin resistance cassette flanking 500 bp upstream and 500 bp downstream region of *gidB* were assembled by overlapping extension PCR for use as an allele exchange substrate (AES),

which was verified by sequencing. WT mc^2-155 and HWS19 transformed with pNIT(kan)::RecET::sacB recombineering plasmid were grown to OD_{600}~0.4, and expression of recET was induced with 10 μM isovaleronitrile (IVN) for 5 h, then competent cells were made by standard methods and transformed with 2 μg of the AES. The cells were recovered for 4 h and selected on LB agar plates containing 20 μg/mL zeocin. The recombinants were confirmed by PCR for verifying the zeocin cassette integration and the appropriate genomic context (Figure S3) (See verification primers sequences in Table S3). *gidB* deletion strains were then cured of the recombinase plasmid prior to further experiments.

For *gidB* complementation construction, several plasmids were constructed. The chromosome integrating mycobacterial plasmid pML1357 (Addgene #32378) was used as the backbone vector. The hygromycin resistance cassette was replaced with a kanamycin resistance cassette and streptomycin resistance cassette as pKML1357 and pSML1357 respectively. *gidB* from wild-type *M. smegmatis* with and without native promoter were amplified and cloned into integrative plasmids pKML1357/ pSML1357 to construct pKML1357-Pnative_*gidB*, pKML1357-Psmyc_*gidB*, pSML1357-Pnative-*gidB*. Then the plasmids were transformed into Δ*gidB* strains and selected onto LB agar with corresponding antibiotics for *gidB* complementation strains. Δ*gidB*::Pnative_*gidB* (KanR) strains were used for dual luciferase mistranslation assay when measuring N to D and Q to E mistranslation rates. Δ *gidB*::Psmyc_*MsmgidB* (KanR) were used for the dual-fluorescence mistranslation assay. Δ*gidB*::Pnative_*gidB* (StrepR) strains were used for dual-luciferase mistranslation assays when measuring W to A mistranslation as the pACET-Renilla-Firefly construct carries a kanamycin resistance marker. In addition, *gidB* mRNA levels in *gidB* deletion and complementation strains were verified by RT-qPCR (Figure S3).

Deletion of *gidB* and complementation in *Escherichia coli*

E. coli HK295 was used as *E.coli* wild-type strain – a kind gift from the Beckwith lab [77]. HK295 was transformed with temperature-sensitive pKD46 plasmid (kind gift from Ting Zhu lab). Hygromycin resistance cassette was amplified from pML1357 with primers containing 50bp upstream and 50bp

downstream of *gidB* as AES (50up-hygR-50down) and verified by sequencing. HK295 with pKD46 was cultured at 30℃ overnight and was diluted 100-fold and sub-cultured into 50ml low-salt LB in a 30 ℃ shaker until OD_{600}~0.1, 0.1% arabinose was then added for inducing the expression of recombinase and transferred into 37℃ shaker for 1 hour. Then competent cells were made by standard electro-transformation method and transformed with 2μg AES PCR product. The cells were recovered in 30℃ for 3 hours and selected onto LB agar plates containing 150 μg/ml Hygromycin in 37℃ incubator. The strain construction was then confirmed by PCR (Figure S5) (See verification primers sequences in Table S3). The *gidB* deletion strain was then cured of pKD46 at 42℃ prior to further experiments.

For *gidB* complementation construction, *E. coli gidB* was amplified with primers containing J23100 promoter (Anderson promoter library, http://parts.igem.org/Promoters/Catalog/Anderson) by PCR and was cloned into r6kg-HK022-attp plasmid – a kind gift from Qiong Wu Lab [78] as r6kg-HK022-attp-*gidB*. HK295-Δ*gidB* was transformed with pRPA001 S-IntHK – a kind gift from Qiong Wu Lab [78], from which competent cells were made and it was then transformed with r6kg-HK022-attp-*gidB* followed by recovering at 37 ℃ for 1 hour and selected onto LB agar containing 25μg/mL chloramphenicol. The complementation strain was verified by PCR in terms of the integration and appropriate genome context. In addition, *gidB* mRNA levels in *gidB* deletion and complementation strains were verified by RT-qPCR (Figure S5).

Measuring mistranslation rates with Renilla-Firefly dual-luciferase reporters

For measuring mistranslation rates in *M. smegmatis*, the shuttle plasmids pTetG-Renilla-Firefly (WT), pTetG-Renilla-D120N-Firefly, pTetG-Renilla-E144Q-Firefly under control of a tetracycline-inducible promoter were used as previously [17]. For measurement of tryptophan to alanine mistranslation rates, the mycobacterial chromosome integrating plasmid pACET-Renilla-Firefly, where expression of the reporter is under control of an acetamide-inducible promoter was used [17]. The *Renilla* gene was mutated by site-directed mutagenesis to Renilla-A214W. For measuring mistranslation rates in *E.coli*,

pEK4 (WT) was used – a kind gift from Philip Farabaugh lab [37]. pEK4-Ren-D120N and pEK4-Ren-E144Q were constructed by site-directed mutagenesis. In all cases, the dual-luciferase kit (Promega, Cat# E1910) was used for measuring Renilla and Firefly luciferase activity.

In mycobacteria, the assay was performed as previously [12]. Briefly, strains with pTetG-Renilla-Firely were cultured to OD600>3, and diluted to OD600~0.2 into fresh 7H9 medium supplemented with 50μg/ml hygromycin and 100 ng /ml anhydrotetracycline for inducing dual luciferase. After 7-8 hours, cells were collected by centrifugation at 12000rpm for 3min, lysed with 40μL passive lysis buffer in 96-well white flat bottom plate for 20-30min (plate shaking at 400rpm, room temperature), then reacted with 50μL substrate Firefly reagents, 360rpm shaked 5s followed by measuring the Firefly luminescence by Fluoroskan Ascent FL luminometer with 1000ms integration time. Then 50μL Stop&Glo reagent was added followed by measuring the Renilla luminescence immediately. For strains with pACET-Renilla-Firely and pTet-$tRNA_{CCA}^{Ala}$ [17], the strains in experimental group were diluted to OD600~0.2 into fresh 7H9 medium supplemented with 50μg/ml hygromycin, 20% acetamide and 100ng/mL anhydrotetracycline for inducing dual luciferase and $tRNA_{CCA}^{Ala}$ respectively. The later procedures were same as above. The corrected Renilla/Firefly representing the mistranslation level is calculated as follows: Corrected Renilla / Firefly (N to D) = $\frac{Renilla(D120N)/Firefly}{Renilla(WT)/Firefly}$, Corrected Renilla / Firefly (Q to E) = $\frac{Renilla(E144Q)/Firefly}{Renilla(WT)/Firefly}$, Corrected Renilla / Firefly (W to A)= $\frac{Renilla(A214W)/Firefly}{Renilla(WT)/Firefly}$.

In *E. coli*, HK295 and its derivatives with pBAD43-*Bs.gltX* (or pBAD-*Dr.AspRS* or pBAD-empty) and pEK4-RenFF WT (or D120N or E144Q) (kind gift from Philip Farabaugh Lab) [37] were cultured overnight. The cells were diluted 1000-fold and sub-cultured into fresh LB supplemented with 0.1% arabinose, 100μg/mL spectinomycin, 100μg/mL ampicillin for 3 hours, then 1mM IPTG was added for inducing dual-luciferase. After 1.5 hours, cells were collected, lysed, reacted with substrate reagents, using the protocol above with the exception that lysis duration was 15min. Luminescence was measured by Fluoroskan Ascent FL luminometer with 40ms integration time. Data analysis was same as *M. smegmatis*.

Measuring mistranslation rates with dual-fluorescence reporters

The pUVtetOR-GLR (green-linker-red) reporter was adapted as previously [12] with some modifications. Briefly, a mutated green fluorescent protein (E222Q) was fused to wild-type monomeric red fluorescent protein (mRFP) with a flexible GGSGGGGSGGGSSGG linker. A C-terminal tag (AANDENYAAAV) targeting the protein for proteolytic degradation [79] was added by PCR.

The procedure of measuring relative mistranslation rates by flow cytometry was as previously described [12] with some modifications. Strains with pUVtetOR-GLR were cultured to OD600~0.2 and then 100ng/ml ATc was added for inducing dual-fluorescence. After 3 hours, cells were diluted into 1mL PBS to OD600~0.05. The GFP and RFP signals of the sample were collected by flow cytometry (BD LSR Fortressa), being excited/ detected by 488nm/520nm laser line and 561nm/585nm laser line respectively. For the strains after high mistranslating selection: Strains expressing pSML1357-*Aph*_D214N and pUVtetOR-GLR were spread onto LB agar containing 50μg/ml Hygromycin and 2μg/ml Kanamycin as experimental group and LB agar containing only 50μg/ml Hygromycin as control group. After 5 days, colonies were scraped from the plates and cultured into 7H9 with 100ng/ml ATc for 3 hours. The following procedures were same as above. For the strains under rifampicin condition: strains with pUVtetOR-GLR were spread onto LB agar no selection plates and LB agar containing 20μg/ml rifampicin. After 5 days, colonies were then scraped from the plates and cultured into 7H9 with 100ng/ml ATc for 3 hours. The following procedures were same as above. Data were analyzed by FlowJo 10.4 for Windows 10. The gating strategy was as follows: Live bacteria were gated to eliminate debris as P1 based on SSC-A and FSC-A, then stringent gating on single cells was applied using a tandem gating strategy based on FSC-A and FSC-H as P2, subsequently using SSC-A and SSC-H as P3. Single cells with positive red fluorescence were acquired as P4 based on the red fluorescence signal. See Figure S4. Relative mistranslation rates were analysed as a histogram of GFP/ RFP ratio as P5 . The mean values of GFP/RFP ratio were calculated by FlowJo software (Flowjo 10.4 for Windows 10).

Construction of plasmids containing non-discriminatory synthetase

Non-discriminatory glutamyl-synthetase from *Bacillus subtilis* (*Bs. gltX*) and aspartyl-synthetase from *Deinococcus radiodurans* (*Dr. AspRS*) were codon-optimized and synthesized by Genwiz and were cloned into *E. coli* expression vector pBAD43. *Bs.gltX* and *Dr.AspRS* were amplified by primers with 20bp overlap to the vector and ligated to the EcoRI / XbaI-digested-vector respectively using Gibson method (NEB, Cat# E2611) where the inserts were under control of arabinose-inducible promoter.

Rifampicin time-kill curve assay

Wild-type and strain HWS19 *M. smegmatis* were cultured in 7H9 medium until OD600~1. Cells were diluted to OD600~0.3 into fresh 7H9 medium containing 20μg/ml rifampicin and cultured into 37°C, 220rpm shaker. Prior to addition of rifampicin, an aliquot was removed for calculation of cell numbers at time zero. At indicated time points, aliquots were taken, washed 3x in PBS and resuspended in PBS prior to being plated onto LB-agar. At least 3 10-fold dilutions were plated per time point. After 3-5 days, visible colonies were counted. The counts at different time points were normalized by counts at time zero for analysis.

Statistical analysis

All statistical methods are described in figures legends, presented as mean with SD. The p values and statistical significance were calculated using GraphPad prism software (Prism 8 for Mac). Two-tailed unpaired Student's t test was used to compare means between groups. ***$p<0.001$, **$p<0.01$, *$p<0.05$, ns $p>0.05$.

Author contributions

HWS optimised the conditions of and performed the initial screen. ZB performed the majority of experiments with some assistance from JYH. BJ conceived of and supervised the study. ZB and BJ wrote the manuscript with input from the other authors.

Acknowledgements

We would like to thank Yuemeng Chen for construction of the dual-fluorescent reporter and the Tsinghua flow cytometry core for technical assistance. This study was in part funded by grants from the Bill & Melinda Gates Foundation (OPP1109789) and funds from Tsinghua University School of Medicine to BJ and ZB. BJ is a Wellcome Trust Investigator (207487/C/17/Z).

References

1. Mohler, K. and M. Ibba, *Translational fidelity and mistranslation in the cellular response to stress.* Nat Microbiol, 2017. **2**: p. 17117.
2. Zaher, H.S. and R. Green, *Fidelity at the molecular level: lessons from protein synthesis.* Cell, 2009. **136**(4): p. 746-62.
3. Ling, J., P. O'Donoghue, and D. Soll, *Genetic code flexibility in microorganisms: novel mechanisms and impact on physiology.* Nat Rev Microbiol, 2015. **13**(11): p. 707-721.
4. Fan, Y., et al., *Heterogeneity of Stop Codon Readthrough in Single Bacterial Cells and Implications for Population Fitness.* Mol Cell, 2017. **67**(5): p. 826-836 e5.
5. Schwartz, M.H. and T. Pan, *Function and origin of mistranslation in distinct cellular contexts.* Crit Rev Biochem Mol Biol, 2017. **52**(2): p. 205-219.
6. Ribas de Pouplana, L., et al., *Protein mistranslation: friend or foe?* Trends Biochem Sci, 2014. **39**(8): p. 355-62.
7. Drummond, D.A. and C.O. Wilke, *The evolutionary consequences of erroneous protein synthesis.* Nat Rev Genet, 2009. **10**(10): p. 715-24.
8. Reynolds, N.M., et al., *Cell-specific differences in the requirements for translation quality control.* Proc Natl Acad Sci U S A, 2010. **107**(9): p. 4063-8.
9. Evans, C.R., et al., *Errors during Gene Expression: Single-Cell Heterogeneity, Stress Resistance, and Microbe-Host Interactions.* mBio, 2018. **9**(4).
10. Chaudhuri, S., et al., *Kasugamycin potentiates rifampicin and limits emergence of resistance in Mycobacterium tuberculosis by specifically decreasing mycobacterial mistranslation.* Elife, 2018. **7**.
11. Rathnayake, U.M., W.N. Wood, and T.L. Hendrickson, *Indirect tRNA aminoacylation during accurate translation and phenotypic mistranslation.* Curr Opin Chem Biol, 2017. **41**: p. 114-122.
12. Su, H.W., et al., *The essential mycobacterial amidotransferase GatCAB is a modulator of specific translational fidelity.* Nat Microbiol, 2016. **1**(11): p. 16147.
13. Schwartz, M.H., et al., *Global tRNA misacylation induced by anaerobiosis and antibiotic exposure broadly increases stress resistance in Escherichia coli.* Nucleic Acids Res, 2016.
14. Schwartz, M.H. and T. Pan, *Temperature dependent mistranslation in a hyperthermophile adapts proteins to lower temperatures.* Nucleic Acids Res, 2016. **44**(1): p. 294-303.
15. Fan, Y., et al., *Protein mistranslation protects bacteria against oxidative stress.* Nucleic Acids Res, 2015. **43**(3): p. 1740-8.
16. Lee, J.Y., et al., *Promiscuous methionyl-tRNA synthetase mediates adaptive mistranslation to protect cells against oxidative stress.* J Cell Sci, 2014. **127**(Pt 19): p. 4234-45.
17. Javid, B., et al., *Mycobacterial mistranslation is necessary and sufficient for rifampicin phenotypic resistance.* Proc Natl Acad Sci U S A, 2014. **111**(3): p. 1132-7.
18. Miranda, I., et al., *Candida albicans CUG mistranslation is a mechanism to create cell surface variation.* MBio, 2013. **4**(4).
19. Li, L., et al., *Naturally occurring aminoacyl-tRNA synthetases editing-domain mutations that cause mistranslation in Mycoplasma parasites.* Proc Natl Acad Sci U S A, 2011. **108**(23): p. 9378-83.
20. Netzer, N., et al., *Innate immune and chemically triggered oxidative stress modifies translational fidelity.* Nature, 2009. **462**(7272): p. 522-6.
21. Ling, J., et al., *Protein aggregation caused by aminoglycoside action is prevented by a hydrogen peroxide scavenger.* Mol Cell, 2012. **48**(5): p. 713-22.
22. Zhang, Y.W., et al., *HspX promotes the polar localization of mycobacterial protein aggregates.* Sci Rep, 2019. **9**(1): p. 14571.
23. Lee, J.W., et al., *Editing-defective tRNA synthetase causes protein misfolding and neurodegeneration.* Nature, 2006. **443**(7107): p. 50-5.

24. Liu, Y., et al., *Deficiencies in tRNA synthetase editing activity cause cardioproteinopathy.* Proc Natl Acad Sci U S A, 2014. **111**(49): p. 17570-5.
25. Kohanski, M.A., et al., *Mistranslation of membrane proteins and two-component system activation trigger antibiotic-mediated cell death.* Cell, 2008. **135**(4): p. 679-90.
26. Fan, Y., et al., *Optimal translational fidelity is critical for Salmonella virulence and host interactions.* Nucleic Acids Res, 2019. **47**(10): p. 5356-5367.
27. Rubio Gomez, M.A. and M. Ibba, *Aminoacyl-tRNA synthetases.* RNA, 2020. **26**(8): p. 910-936.
28. Chong, Y.E., X.L. Yang, and P. Schimmel, *Natural homolog of tRNA synthetase editing domain rescues conditional lethality caused by mistranslation.* J Biol Chem, 2008. **283**(44): p. 30073-8.
29. Vargas-Rodriguez, O. and K. Musier-Forsyth, *Exclusive use of trans-editing domains prevents proline mistranslation.* J Biol Chem, 2013. **288**(20): p. 14391-9.
30. LaRiviere, F.J., A.D. Wolfson, and O.C. Uhlenbeck, *Uniform binding of aminoacyl-tRNAs to elongation factor Tu by thermodynamic compensation.* Science, 2001. **294**(5540): p. 165-8.
31. Morse, J.C., et al., *Elongation factor-Tu can repetitively engage aminoacyl-tRNA within the ribosome during the proofreading stage of tRNA selection.* Proceedings of the National Academy of Sciences, 2020. **117**(7): p. 3610-3620.
32. Ruan, B., et al., *Quality control despite mistranslation caused by an ambiguous genetic code.* Proc Natl Acad Sci U S A, 2008. **105**(43): p. 16502-7.
33. Sheppard, K. and D. Soll, *On the evolution of the tRNA-dependent amidotransferases, GatCAB and GatDE.* J Mol Biol, 2008. **377**(3): p. 831-44.
34. Manickam, N., et al., *Studies of translational misreading in vivo show that the ribosome very efficiently discriminates against most potential errors.* RNA, 2014. **20**(1): p. 9-15.
35. Curnow, A.W., et al., *Glu-tRNAGln amidotransferase: a novel heterotrimeric enzyme required for correct decoding of glutamine codons during translation.* Proc Natl Acad Sci U S A, 1997. **94**(22): p. 11819-26.
36. Cai, R.J., et al., *Forward Genetics Reveals a gatC-gatA Fusion Polypeptide Causes Mistranslation and Rifampicin Tolerance in Mycobacterium smegmatis.* Front Microbiol, 2020. **11**: p. 577756.
37. Kramer, E.B. and P.J. Farabaugh, *The frequency of translational misreading errors in E. coli is largely determined by tRNA competition.* RNA, 2007. **13**(1): p. 87-96.
38. Leng, T., et al., *Translational misreading in Mycobacterium smegmatis increases in stationary phase.* Tuberculosis (Edinb), 2015. **95**(6): p. 678-81.
39. Chen, Y.X., et al., *Measurement of Specific Mycobacterial Mistranslation Rates with Gain-of-function Reporter Systems.* J Vis Exp, 2019(146).
40. Okamoto, S., et al., *Loss of a conserved 7-methylguanosine modification in 16S rRNA confers low-level streptomycin resistance in bacteria.* Mol Microbiol, 2007. **63**(4): p. 1096-106.
41. Wong, S.Y., et al., *Functional role of methylation of G518 of the 16S rRNA 530 loop by GidB in Mycobacterium tuberculosis.* Antimicrob Agents Chemother, 2013. **57**(12): p. 6311-8.
42. Boehr, D.D., P.R. Thompson, and G.D. Wright, *Molecular mechanism of aminoglycoside antibiotic kinase APH(3')-IIIa: roles of conserved active site residues.* J Biol Chem, 2001. **276**(26): p. 23929-36.
43. Hon, W.C., et al., *Structure of an enzyme required for aminoglycoside antibiotic resistance reveals homology to eukaryotic protein kinases.* Cell, 1997. **89**(6): p. 887-95.
44. Zhu, J.H., et al., *Rifampicin can induce antibiotic tolerance in mycobacteria via paradoxical changes in rpoB transcription.* Nat Commun, 2018. **9**(1): p. 4218.
45. Chong, Y.E., et al., *Distinct ways of G:U recognition by conserved tRNA binding motifs.* Proc Natl Acad Sci U S A, 2018. **115**(29): p. 7527-7532.
46. Hou, Y.M. and P. Schimmel, *A simple structural feature is a major determinant of the identity of a transfer RNA.* Nature, 1988. **333**(6169): p. 140-5.
47. Swairjo, M.A., et al., *Alanyl-tRNA synthetase crystal structure and design for acceptor-stem recognition.* Mol Cell, 2004. **13**(6): p. 829-41.

561 48. Wang, B.W., J.H. Zhu, and B. Javid, *Clinically relevant mutations in mycobacterial LepA cause*
562 *rifampicin-specific phenotypic resistance.* Sci Rep, 2020. **10**(1): p. 8402.
563 49. Vijay, S., et al., *Most-probable number based minimum duration of killing assay for*
564 *determining the spectrum of rifampicin susceptibility in clinical M. tuberculosis isolates.*
565 Antimicrob Agents Chemother, 2020.
566 50. Safi, H., et al., *Phase variation in Mycobacterium tuberculosis glpK produces transiently*
567 *heritable drug tolerance.* Proc Natl Acad Sci U S A, 2019. **116**(39): p. 19665-19674.
568 51. Hicks, N.D., et al., *Clinically prevalent mutations in Mycobacterium tuberculosis alter*
569 *propionate metabolism and mediate multidrug tolerance.* Nat Microbiol, 2018. **3**(9): p. 1032-
570 1042.
571 52. Vilcheze, C., et al., *Enhanced respiration prevents drug tolerance and drug resistance in*
572 *Mycobacterium tuberculosis.* Proc Natl Acad Sci U S A, 2017. **114**(17): p. 4495-4500.
573 53. Gold, B. and C. Nathan, *Targeting Phenotypically Tolerant Mycobacterium tuberculosis.*
574 Microbiol Spectr, 2017. **5**(1).
575 54. Richardson, K., et al., *Temporal and intrinsic factors of rifampicin tolerance in mycobacteria.*
576 Proc Natl Acad Sci U S A, 2016. **113**(29): p. 8302-7.
577 55. Brauner, A., et al., *Distinguishing between resistance, tolerance and persistence to antibiotic*
578 *treatment.* Nat Rev Microbiol, 2016. **14**(5): p. 320-30.
579 56. Abel Zur Wiesch, P., et al., *Classic reaction kinetics can explain complex patterns of antibiotic*
580 *action.* Sci Transl Med, 2015. **7**(287): p. 287ra73.
581 57. Aldridge, B.B., I. Keren, and S.M. Fortune, *The Spectrum of Drug Susceptibility in Mycobacteria.*
582 Microbiol Spectr, 2014. **2**(5).
583 58. Wakamoto, Y., et al., *Dynamic persistence of antibiotic-stressed mycobacteria.* Science, 2013.
584 **339**(6115): p. 91-5.
585 59. Tollerson, R., 2nd and M. Ibba, *Translational regulation of environmental adaptation in*
586 *bacteria.* J Biol Chem, 2020. **295**(30): p. 10434-10445.
587 60. Shippy, D.C. and A.A. Fadl, *RNA modification enzymes encoded by the gid operon: Implications*
588 *in biology and virulence of bacteria.* Microb Pathog, 2015. **89**: p. 100-7.
589 61. Stojkovic, V. and D.G. Fujimori, *Mutations in RNA methylating enzymes in disease.* Curr Opin
590 Chem Biol, 2017. **41**: p. 20-27.
591 62. Pape, T., W. Wintermeyer, and M.V. Rodnina, *Complete kinetic mechanism of elongation*
592 *factor Tu-dependent binding of aminoacyl-tRNA to the A site of the E. coli ribosome.* EMBO J,
593 1998. **17**(24): p. 7490-7.
594 63. Zaher, H.S. and R. Green, *Quality control by the ribosome following peptide bond formation.*
595 Nature, 2009. **457**(7226): p. 161-6.
596 64. Dale, T. and O.C. Uhlenbeck, *Binding of misacylated tRNAs to the ribosomal A site.* RNA, 2005.
597 **11**(11): p. 1610-5.
598 65. Dale, T., et al., *Specificity of the ribosomal A site for aminoacyl-tRNAs.* Nucleic Acids Res, 2009.
599 **37**(4): p. 1202-10.
600 66. Effraim, P.R., et al., *Natural amino acids do not require their native tRNAs for efficient selection*
601 *by the ribosome.* Nat Chem Biol, 2009. **5**(12): p. 947-53.
602 67. Schuwirth, B.S., et al., *Structural analysis of kasugamycin inhibition of translation.* Nat Struct
603 Mol Biol, 2006. **13**(10): p. 879-86.
604 68. van Buul, C.P., W. Visser, and P.H. van Knippenberg, *Increased translational fidelity caused by*
605 *the antibiotic kasugamycin and ribosomal ambiguity in mutants harbouring the ksgA gene.*
606 FEBS Lett, 1984. **177**(1): p. 119-24.
607 69. Bullwinkle, T.J., et al., *Oxidation of cellular amino acid pools leads to cytotoxic mistranslation*
608 *of the genetic code.* Elife, 2014. **3**.
609 70. Chen, Y.X., et al., *Selective translation by alternative bacterial ribosomes.* Proc Natl Acad Sci U
610 S A, 2020. **117**(32): p. 19487-19496.

611 71. Kurylo, C.M., et al., *Endogenous rRNA Sequence Variation Can Regulate Stress Response Gene*
612 *Expression and Phenotype.* Cell Rep, 2018. **25**(1): p. 236-248 e6.
613 72. Parks, M.M., et al., *Variant ribosomal RNA alleles are conserved and exhibit tissue-specific*
614 *expression.* Sci Adv, 2018. **4**(2): p. eaao0665.
615 73. Emmott, E., M. Jovanovic, and N. Slavov, *Ribosome Stoichiometry: From Form to Function.*
616 Trends Biochem Sci, 2019. **44**(2): p. 95-109.
617 74. Dinman, J.D., *Pathways to Specialized Ribosomes: The Brussels Lecture.* J Mol Biol, 2016.
618 **428**(10 Pt B): p. 2186-94.
619 75. Sloan, K.E., et al., *Tuning the ribosome: The influence of rRNA modification on eukaryotic*
620 *ribosome biogenesis and function.* RNA Biology, 2017. **14**(9): p. 1138-1152.
621 76. Snapper, S.B., et al., *Isolation and characterization of efficient plasmid transformation mutants*
622 *of Mycobacterium smegmatis.* Mol Microbiol, 1990. **4**(11): p. 1911-9.
623 77. Kadokura, H. and J. Beckwith, *Four cysteines of the membrane protein DsbB act in concert to*
624 *oxidize its substrate DsbA.* EMBO J, 2002. **21**(10): p. 2354-63.
625 78. Yao, Y., et al., *A Direct RNA-to-RNA Replication System for Enhanced Gene Expression in*
626 *Bacteria.* ACS Synth Biol, 2019. **8**(5): p. 1067-1078.
627 79. Andersen, J.B., et al., *New unstable variants of green fluorescent protein for studies of*
628 *transient gene expression in bacteria.* Appl Environ Microbiol, 1998. **64**(6): p. 2240-6.

629

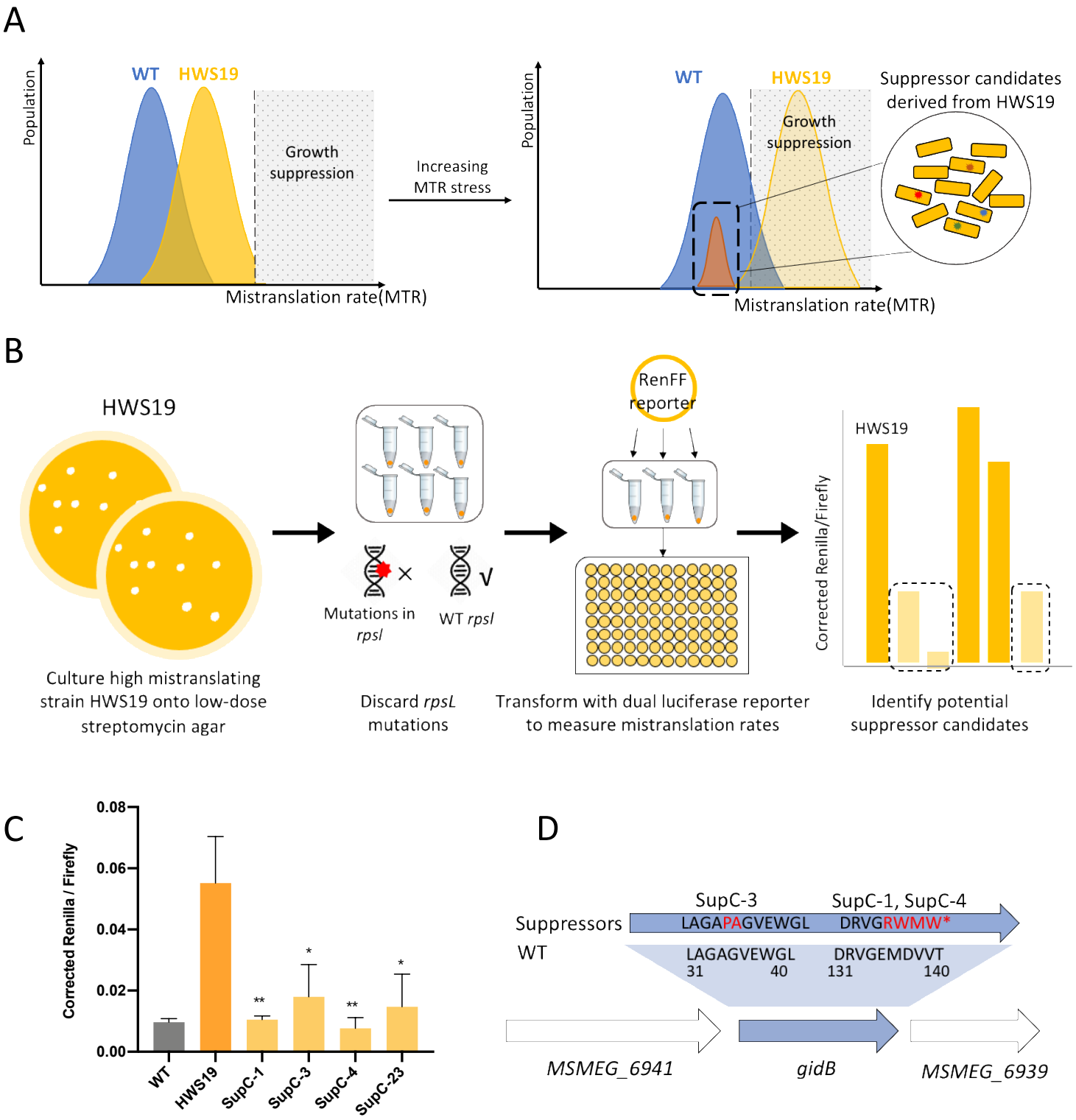

Figure 1. A suppressor screen identifies *gidB* as a potential translational fidelity factor. (A) Schematic of principle for the suppressor screen: Excess mistranslation results in growth suppression. Culture of high mistranslating strain HWS19 under conditions that increases mistranslation rates selects for mutations that increase translational fidelity to levels similar to wild-type bacteria. **(B)** Cartoon outline of the screen: Strain HWS19 was cultured on low-dose streptomycin agar to select low mistranslating mutants. Streptomycin-resistant mutants were discarded before transforming survivors with dual luciferase mistranslation reporter to identify potential suppressors. **(C)** Corrected Renilla/firefly (measuring asparagine to aspartate mistranslation) of wild-type, HWS19 and suppressor mistranslation rates. **(D)** Cartoon mapping location of mutations in *gidB* from 3 suppressor candidates.

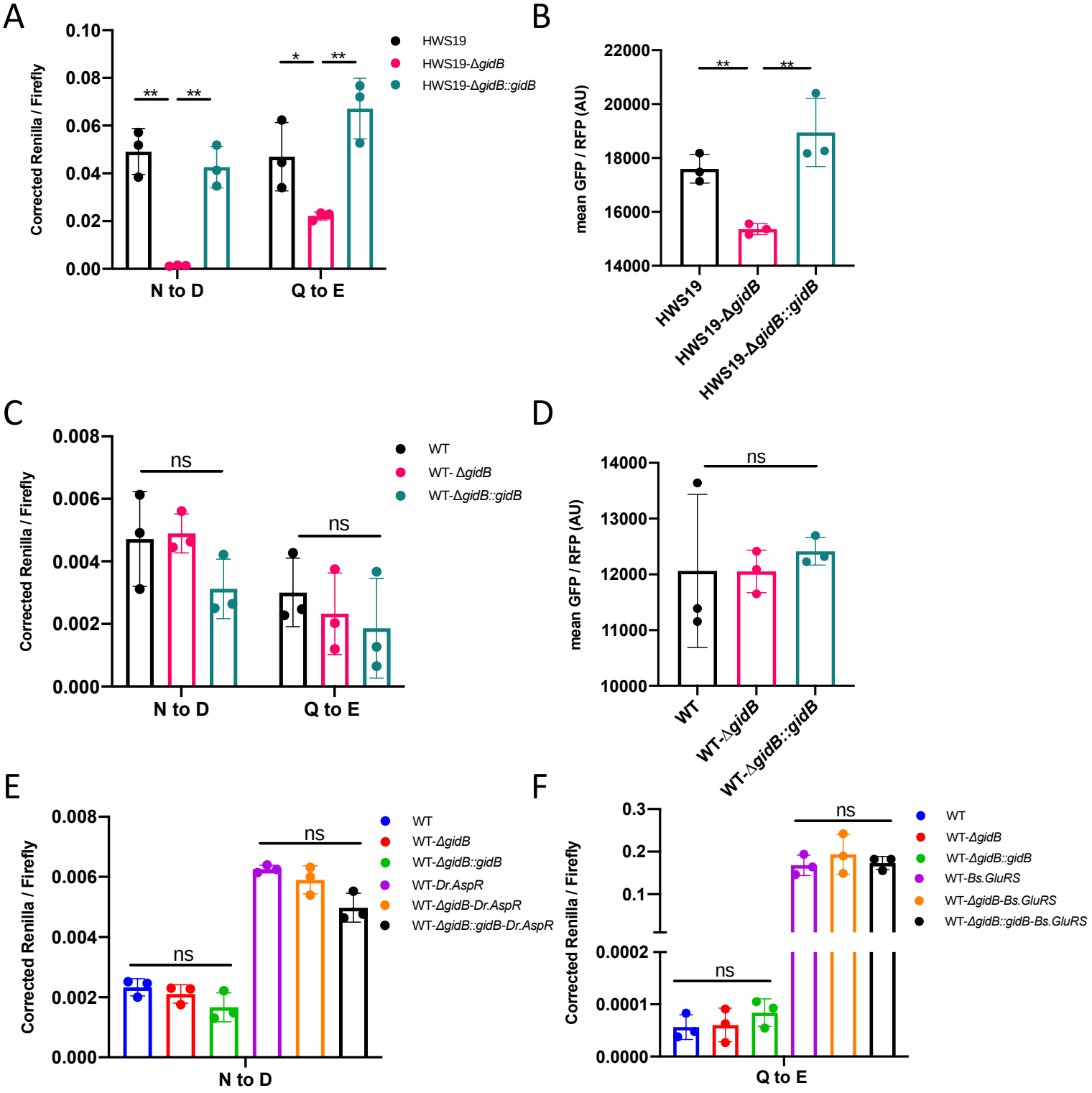

Figure 2. Deletion of *gidB* increases discrimination against misacylated tRNA in mycobacteria with high mistranslation. (A) Measurement of asparagine to aspartate and glutamine to glutamate mistranslation rates using dual-luciferase reporters in strains HWS19, HWS19Δ*gidB* and HWS19Δ*gidB* ::*gidB.* **(B)** measurement of glutamine to glutamate mistranslation rates using a dual-fluorescent reporter in strains HWS19, HWS19Δ*gidB* and HWS19Δ*gidB* ::*gidB.* **(C)** and **(D)** Same as (A) and (B) respecticely but with strains WT, WTΔ*gidB* and WTΔ*gidB*::*gidB M. smegmatis.* Measurement of asparagine to aspartate **(E)** and glutamine to glutamate **(F)** mistranslation rates using dual-luciferase reporters in WT, Δ*gidB*, complemented (Δ*gidB*::*gidB*) *E. coli*, and upon induction of non-discriminatory aspartyl (WT-*Dr AspR*) and non-discriminatory glutamyl (WT-*Bs GluRS*) aminoacyl synthetases, with *gidB* deletion and complementation. In all cases, 3 biological replicates per condition. *p<0.05, **p<0.01, ***p<0.001, ns p>0.05 by Student's t-test).

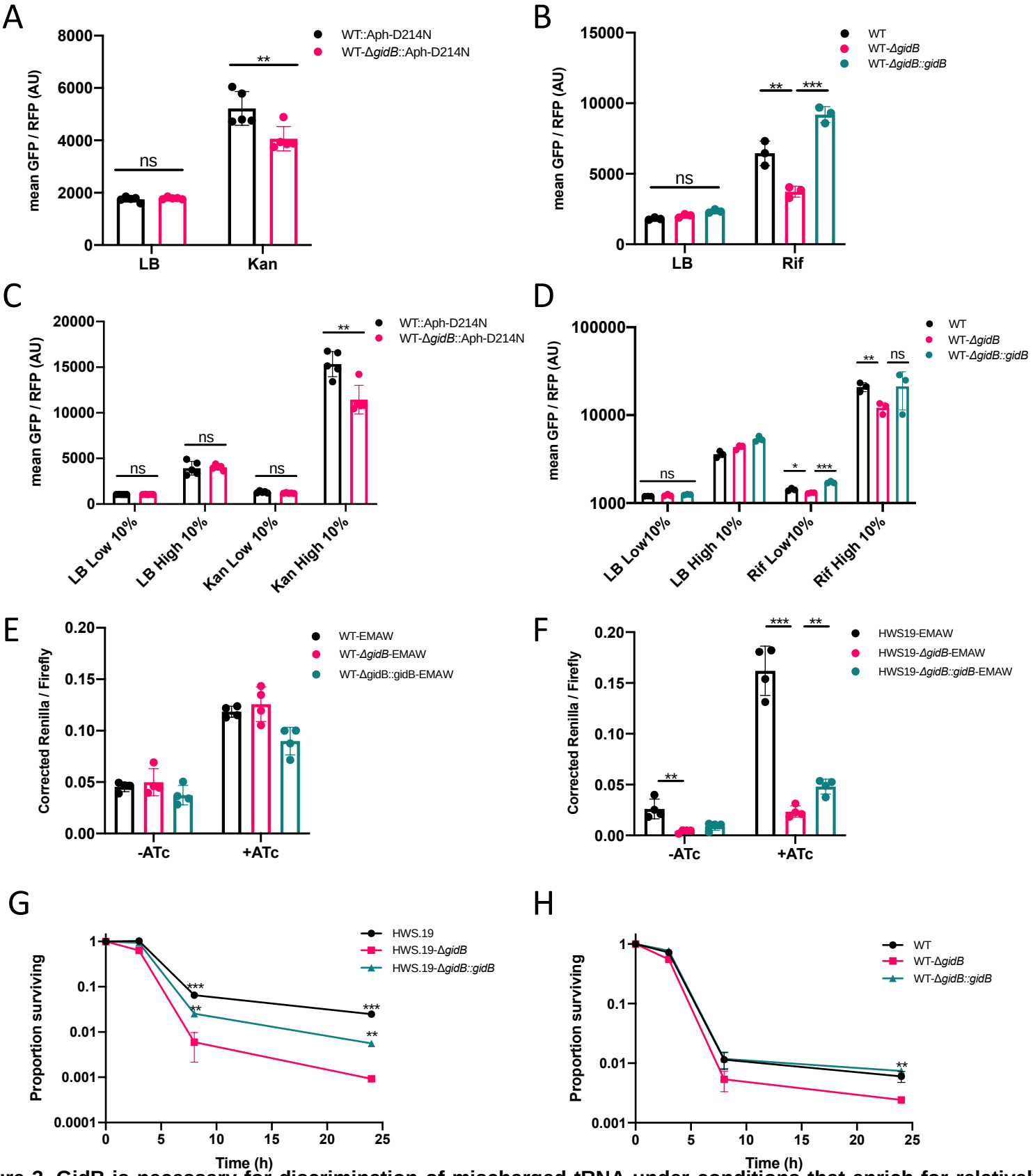

Figure 3. GidB is necessary for discrimination of mischarged tRNA under conditions that enrich for relatively high mistranslation rates. (A) Measurement of glutamine to glutamate mistranslation rates using dual-fluorescent reporter in WT and *gidB*-deleted *M. smegmatis* expressing Aph-D214N reporter isolated from LB-agar (LB) or 2µg/mL kanamycin-agar (Kan). **(B)** Same as (A) but with WT, *gidB*-deleted and complemented strains isolated from LB-agar (LB) or 20µg/mL rifampicin-agar (Rif). **(C)** and **(D)** analysis of data in (A) and (B) respectively, but selectively gating only on the bacterial population with the lowest (low 10%) and highest (high 10%) GFP/RFP ratios representing mistranslation rates. **(E)** Measurement of tryptophan to alanine mistranslation rates using dual-luciferase reporter of WT, *gidB*-deleted and complemented *M. smegmatis* expressing $tRNA_{CCA}^{Ala}$ (EMAW) in absence (-Atc) and presence (+ATc) of anhydrotetracycline to induce expression of the tRNA. **(F)** Same as (E) but on HWS19 background. Time-kill to rifampicin (20µg/m) survival graph of *M. smegmatis*, *gidB*-deleted and complemented *M. smegmatis* on WT **(G)** and HWS19 **(H)** strain backgrounds. Mean of biological replicates (>3) +/- SD shown in each panel. *p<0.05, **p<0.01, ***p<0.001, ns p>0.05 by Student's t-test).